Surface-water transport of suspended matter through wetland vegetation of the Florida everglades

James E. Saiers,[1] Judson W. Harvey,[2] and Steven E. Mylon[1]

Received 9 July 2003; revised 28 August 2003; accepted 4 September 2003; published 7 October 2003.

[1] The mobility of waterborne particulate matter plays an important role in the water quality, landscape evolution, and ecology of freshwater wetlands. In this work, we measured the surface-water transport of inorganic particles in a tracer experiment at a wetland in the Florida Everglades. Comparison of the results of this experiment to calculations of a three-dimensional transport model shows that dispersive mixing was small and that rate-limited mass-transfer reactions with emergent vegetation and periphyton substantially reduced water-column concentrations of particles. *INDEX TERMS:* 1871 Hydrology: Surface water quality; 1890 Hydrology: Wetlands; 1806 Hydrology: Chemistry of fresh water. **Citation:** Saiers, J. E., J. W. Harvey, and S. E. Mylon, Surface-water transport of suspended matter through wetland vegetation of the Florida everglades, *Geophys. Res. Lett.*, *30*(19), 1987, doi:10.1029/2003GL018132, 2003.

1. Introduction

[2] The transport of particulate matter is critical to the functioning of freshwater wetlands. Microscopic waterborne particles, such as colloid-sized mineral precipitates and colloidal organic matter, are capable of binding a variety of contaminants, and these contaminant-particle interactions influence contaminant bioavailability and movement [e.g., *Schulz and Peall*, 2001]. Besides affecting contaminant migration, particle transport processes contribute to changes in wetland geomorphology. In the Florida Everglades, for example, the degradation of the highly organized ridge and slough landscape is believed to arise, in part, from disruption of natural surface-water flow patterns, which has led to increased deposition of suspended matter in the sloughs [*Aumen*, 2003]. Particle transport phenomena also have implications to the distribution of wetland vegetation that rely on surface-water currents for seed dispersal [e.g., *Middleton*, 2000].

[3] Despite the importance of mobile particulates to the water quality, geomorphology, and ecological functioning of wetlands, field-based observations are too scarce to permit quantitative inferences to be made regarding particle-transport characteristics within freshwater wetlands. We begin to fill this gap in knowledge by measuring the movement of particulate matter in a tracer-injection experiment conducted in the Florida Everglades. Our analysis of these data reveals how advection, dispersion, and interception by aquatic vegetation combine to influence particle mobility.

2. Site Description

[4] The particle tracer experiment was performed at a surface-water flume facility constructed within Shark River Slough (25°38′31.2″N, 80°43′20.4″W) in Everglades National Park. The flume facility, originally designed to monitor wetland response to low-level additions of phosphorus, has four open-ended channels, each 3 m wide and extending for 100 m in a southerly direction. Our experiment was conducted in the westernmost channel on 21 November 2002, when the depth of water equaled 60 cm. Phosphorous dosing in this channel started prior to our particle-tracer experiment and increased water-column concentrations of phosphorus at the head of the channel (where phosphorus was added) to 15 μg/L. Surface water collected from the channel contained high concentrations of dissolved organic carbon (14 mg/L) and had a pH and ionic strength of 6.9 and 0.004 M, respectively. *Eleocharis cellulosa* (806 stems/m^2) and *Eleocharis elongata* (341 stems/m^2) composed the dominant macrophytes in the channel (*E. Gaiser, unpublished data*, 2002), and periphyton (a matrix of algae and heterotrophic microbes) persisted as a discontinuous mat floating on the top few centimeters of the water column and as thin coatings (''sweaters'') on macrophyte stems. The macrophytes were anchored in peat, which was approximately 0.5 m in thickness and underlain by limestone. Directly above the peat was a thin layer (0.04 m) of flocculent detrital organic matter.

3. Experimental Methodology

[5] Particles composed of titanium dioxide (TiO_2) with an average diameter of 0.3 μm were suspended in filtered (0.2 μm) Everglades water and used as the tracer. Background concentrations of TiO_2 in Shark River Slough are low, so the TiO_2 tracer particles could be distinguished from the autochthonous particles on the basis of their chemical signature.

[6] We introduced a 9 g/L TiO_2 suspension 0.7 m upgradient of the leading edge of the vegetation, which was located approximately 10 m from the head of the channel (Figure 1a). The injection was accomplished by using a metering pump to deliver the TiO_2 tracer at constant rate (100 mL/min) through a slotted hose that spanned the central 1.8 m of the channel and rested 24 cm below the water surface (Figure 1b). The duration of the injection was 0.9 hours. Sampling for the TiO_2 began before the start of the injection and continued for 3 hours after its termination. Water samples (20 mL) were repeat-

[1]School of Environmental Studies, Yale University, New Haven, Connecticut, USA.
[2]U.S.G.S., Reston, Virginia, USA.

0094-8276/03/2003GL018132$05.00

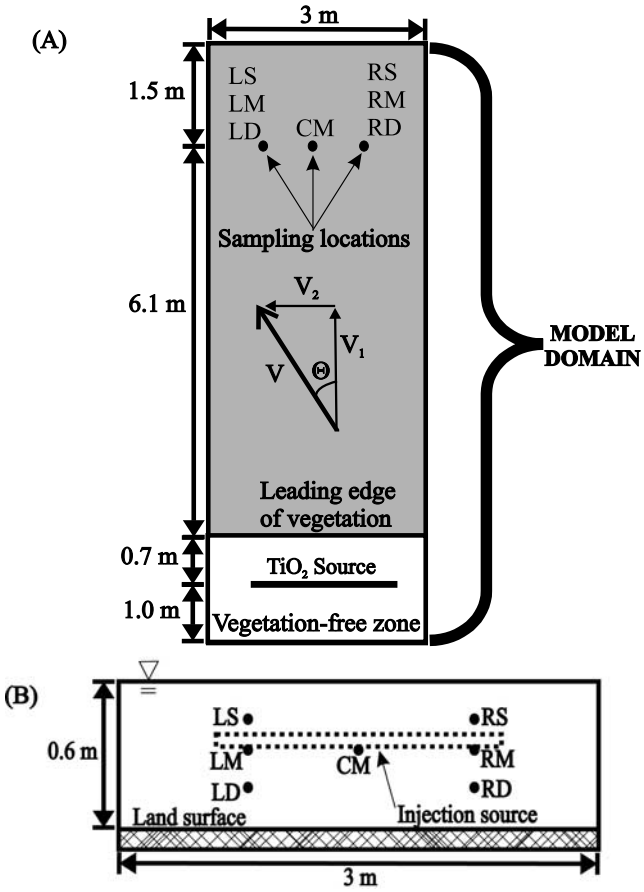

Figure 1. (a) Plan-view positions of the tracer-injection source and samplers within the portion of the channel used for the particle-tracer experiment. The model domain is situated near the head of the 100-m long channel. (b) Cross-sectional positions of the tracer-injection source and samplers as viewed from the head of the channel.

edly collected in plastic scintillation vials by applying suction to 1/8″ stainless steel sampling tubes installed at discrete points located 6.8 m down channel from the injection (Figures 1a and 1b). The sampling points were designated as LS, LM, LD, CM, RS, RM, and RD, where L (left), C (center), and R (right) delineate lateral position and refer to locations 0.8 m inside the left wall, at the channel center, and 0.8 m inside the right wall, respectively, and S (shallow), M (mid-depth), and D (deep) delineate vertical position and refer to depths of 0.15, 0.27, and 0.42 m, respectively. Concentrations of titanium (Ti) in the surface-water samples were measured in the laboratory by inductively coupled plasma mass spectrometry following acid dissolution of the TiO_2 particles.

4. Mathematical Model

[7] We quantified particle advection, dispersion, and immobilization kinetics by comparing measured TiO_2 breakthrough curves to those calculated by a mathematical model. The model solves an equation that accounts for coupled advective-dispersive transport and rate-limited mass transfer in a domain of constant water depth, where particle dispersion is anisotropic and the mean flow velocity is uniform (i.e., independent of position) and in the direction parallel to the x axis of the coordinate system:

$$\frac{\partial C}{\partial t} = \frac{\partial}{\partial x}\left[D_{Lon}\frac{\partial C}{\partial x}\right] + \frac{\partial}{\partial y}\left[D_{Lat}\frac{\partial C}{\partial y}\right] + \frac{\partial}{\partial z}\left[D_V\frac{\partial C}{\partial z}\right] - V\frac{\partial C}{\partial x} - \lambda C \quad (1)$$

where C is particle concentration, D_{Lon}, D_{Lat}, and D_V are the longitudinal, lateral, and vertical dispersion coefficients, respectively, V is the mean surface-water velocity, and λ is a mass-transfer coefficient for particle immobilization. Interception by aquatic vegetation and adsorption of particles that diffused to the sediment were among the plausible mechanisms of particle immobilization in our experiment; however, sedimentation did not contribute significantly to TiO_2 removal because the settling velocity of these particles was very small ($<10^{-2}$ cm/h).

[8] We employed a finite-element method to solve equation (1) for a three-dimensional domain measuring 9.3 m long, 3 m wide (the channel width), and 0.6 m deep (Figure 1a). The model domain was discretized into 16,000 quadratic-Lagrange elements and the numerical solution to equation (1) was obtained for zero initial TiO_2 concentrations, a zero gradient in TiO_2 concentrations across the lateral boundaries, and zero total flux across both the free surface and ground surface. A specified TiO_2 flux across a planar internal boundary (0.05 m $\times$ 1.8 m) was used to simulate the injection source (Figures 1a and 1b).

[9] Observations from a separate experiment on the transport of bromide (a conservative tracer) revealed that the channel walls were permeable and that a cross-channel component of surface-water flow existed. While the bromide data could not be used to make quantitative determinations about TiO_2 transport (because the magnitude of the flow velocities varied between experiments), the bromide results did emphasize the need to account for cross-channel flow within our modeling framework. We accomplished this by computing the magnitude and direction of the mean surface-water velocity from the component velocities and then we rotated the coordinate system for the model domain such that the x axis was parallel with the direction of V. The magnitude and direction of the mean surface-water velocity are expressed by

$$V = \left(v_1^2 + v_2^2\right)^{1/2} \quad (2)$$

and

$$\Theta = \tan^{-1}\left(v_2/v_1\right) \quad (3)$$

where v_1 and v_2 are the components of the surface-water velocity parallel to the channel wall and perpendicular to the channel wall, respectively (Figure 1a).

[10] We applied the model in inverse mode in order to estimate v_1 and v_2, as well as the parameters that govern dispersion (D_{Lon}, D_{Lat}, and D_V) and particle-immobilization kinetics (λ). Best-fit parameter values were identified by using a Levenberg-Marquardt algorithm (as programmed

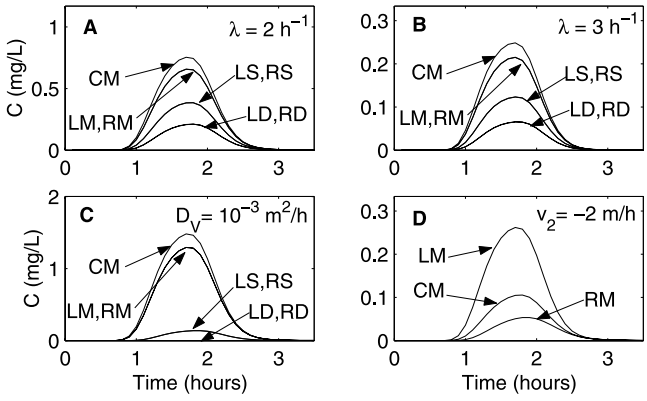

Figure 2. Model-calculated TiO_2 breakthrough curves for (a) base-case parameter values, (b) $\lambda = 3\ h^{-1}$, (c) $D_V = 0.001\ m^2\ h^{-1}$, and (d) $v_2 = -2\ m\ h^{-1}$. (The y-axis scaling varies between plots.) The breakthrough curves are referenced by the lateral and vertical positions of the samplers (see Figure 1b). In D, only breakthrough curves calculated for the mid-depth samplers are shown.

in MATLAB) to minimize the sum-of-the-squared residuals between measured and modeled TiO_2 concentrations.

5. Results

5.1. Model Sensitivity Analysis

[11] We examined the sensitivity of particle breakthrough at the sampling positions to changes in the parameters that govern advection, dispersion, and particle immobilization kinetics. This involved comparing a simulation generated with a base-case set of parameter values to modeled results obtained by individually adjusting λ, D_V, and v_2 from their base-case values of 2 h^{-1}, 0.005 $m^2\ h^{-1}$, and 0 $m\ h^{-1}$, respectively.

[12] Model calculations made with the base-case parameters reveal that particle concentrations for the sampling-site positions on the left side of the channel (i.e., LS, LM, LD) are identical to those computed for corresponding depths on the right side (i.e., RS, RM, RD) (Figure 2a). Three conditions combine to produce this symmetry in particle breakthrough: the left- and right-side sampling sites are spaced equal distances from the channel center, the injection source is centered laterally within the channel, and the flow field parallels the channel walls (i.e., $V = v_1$ and $\Theta = 0°$). Peak breakthrough concentrations at the mid-depth samplers are greatest at the central sampling point (CM) and decrease towards the left (LM) and right (RM) owing to dilution by lateral dispersion. On both the left and right sides of the channel, breakthrough concentrations decline with vertical distance away from the injection source (see Figure 1B for sampler depths); that is, concentrations at the mid-depth samplers (LM and RM) are higher than concentrations at the shallow samplers (LS and RS), which, in turn, are higher than those at the deep samplers (LD and RD) (Figure 2a).

[13] Variation in the value of λ controls the magnitude of the breakthrough concentrations. An increase in λ from 2 h^{-1} to 3 h^{-1} leads to a 3-fold decline in peak breakthrough (compare Figures 2a and 2b). Changes in λ do not affect the apparent dispersion or travel time of the suspended particles, however. Because the immobilization rate varies linearly with C, increases in λ promote proportionate reductions in breakthrough concentrations at all sampling positions.

[14] The vertical dispersion coefficient (D_V) regulates the distribution in particle concentrations between the mid-depth sampling sites and the shallow and deep sampling sites. Vertical mixing decreases as D_V declines from its base-case value to 0.001 $m^2\ h^{-1}$, so the particles (which were injected near mid depth) do not spread in appreciable concentrations to the shallow and deep sampling sites, and particle transport is relegated to the middle of the water column, resulting in comparatively higher breakthrough concentrations at the mid-depth samplers (compare Figures 2a and 2c).

[15] We adjusted v_2 from its base-case value of zero in order to explore the effects of cross-channel flow on particle breakthrough. For $v_2 = -2\ m\ h^{-1}$ (the negative sign signifies that cross-channel component of flow is from right to left), symmetry in particle breakthrough between the left and right sampling sites disappears and concentrations on the left side of the channel grow at the expense of concentrations on the right side of the channel (compare Figures 2a and 2d). Cross-channel flow also lowers peak breakthrough concentrations because particles exit the channel before being detected at the monitoring points.

5.2. Comparison of Field Observations and Model Calculations

[16] TiO_2 particles appeared at the sampling sites approximately one hour after the injection was initiated (Figure 3). Measured breakthrough concentrations were highest at the mid-depth samplers and, among these samplers, the magnitude of the breakthrough decreased from the left side of the channel (LM), where concentrations peaked at 95 μg/L, to the right side of the channel (RM), where concentrations peaked at 8 μg/L. Concentrations did not exceed background levels at either deep sampler or at the right-side shallow sampler, but breakthrough was apparent at LS.

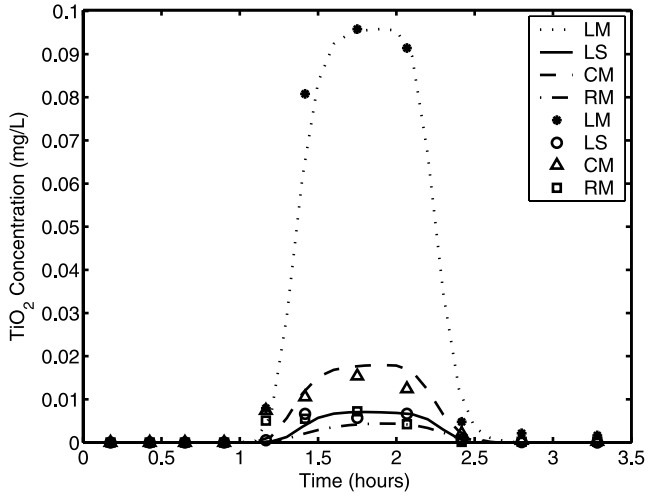

Figure 3. Measured (symbols) and modeled (lines) breakthrough concentrations of TiO_2. Measured and modeled TiO_2 concentrations at LD, RS, and RD remained at baseline levels during the injection and are not shown.

[17] Although deviations between experimental and calculated results exist, the model matches the range in observed breakthrough behavior reasonably well (Figure 3). The best-fit values of v_1 and v_2 are 5.1 and -1.5 m h^{-1}, respectively, which corresponds to a mean surface-water velocity (V) of 5.3 m h^{-1}. The cross-channel component of flow ($\Theta = -16.4°$) leads to the asymmetry in breakthrough concentrations between the left and right sides of the channel.

[18] Dispersion of the TiO_2 particles was small. Best-fit estimates of D_{Lon} and D_{Lat} are nearly equal at 0.16 and 0.15 m^2 h^{-1}, respectively, and $\approx$150 times greater than D_V ($=0.001$ m^2 h^{-1}). The small D_V is consistent with our observations that the TiO_2 plume traveled through the center of the water column and did not spread in substantial levels to the shallow and deep samplers.

[19] The optimal value of λ is 3.55 h^{-1}. Based on this estimate, the time scale for immobilization (λ^{-1}) is 0.3 h, or 4.5 fold less than the time required for particles to be transported by advection from the injection source to the sampler array. The absence of tailing on the experimental breakthrough curves suggests that captured particles were not remobilized during the course of the experiment.

6. Discussion

[20] The mean surface-water velocity estimated from our experiment is 5.3 m h^{-1}, which, for the average stem diameter measured within the channel (0.2 cm), corresponds to a stem Reynolds Numbers ($Re_s = Vd/\nu$, where ν is the kinematic viscosity and d is stem diameter) of approximately 3. This value is more than an order of magnitude less than Re_s values reported for studies conducted with dissolved tracers in tidal marshes or in laboratory flumes containing model vegetation [*Leonard and Luther*, 1995; *Nepf et al.*, 1997a] and indicates that flow velocities in our experiment were too small to generate turbulence within stem wakes. Given that stem wakes dominate turbulence production in wetland environments [*Nepf*, 1999], these results imply that turbulent mixing of the TiO_2 particles was insignificant.

[21] For the low-Re_s flow observed in this study, the stem-wake structure is laminar and particle-spreading rates reflect contributions of Brownian diffusion, bed-induced shear, and mechanical dispersion. Brownian diffusion played a negligible role in dispersive mixing within the channel, as the Brownian diffusion coefficient for the TiO_2 particles ($=5 \times 10^{-9}$ m^2 h^{-1}) is several orders of magnitude lower than the best-fit estimates of D_{Lon}, D_{Lat}, and D_V. Like Brownian diffusion, boundary-induced shear flow was not an important contributor to particle dispersion because, within aquatic vegetation, gradients in velocity attributable to retardation of flow near the bed surface are restricted to a narrow region (i.e., 1–2 cm) adjacent to the bed [*Nepf et al.*, 1997b]. This boundary layer lies well below the portion of the water column sampled by the TiO_2 tracer cloud. Mechanical dispersion, or mixing caused by local variations in the direction and velocity of flow around the mean velocity (V), represented the dominant mechanism of TiO_2-particle dispersal. The local variations in advective transport that promote mechanical dispersion are not caused by turbulence, but arise from small-scale heterogeneity in the density of vegetation and resulting nonuniformities in flow resistance and tortuosity of particle-transport pathways [see *Nepf et al.*, 1997b].

[22] Mechanical dispersion was anisotropic in our experiment, with spreading in the longitudinal and lateral directions exceeding dispersion in the vertical direction by more than two orders of magnitude. The comparatively small vertical dispersion is consistent with observations of solute transport through geologic environments, which, like wetland systems, are composed of tortuous transport pathways, and suggests that vertical variation in vegetative structure is considerably less than that in the horizontal directions. These results also indicate that vertical mixing of particles is exceedingly slow in the absence of strong winds, thermal overturn, or other conditions that could promote turbulence. In our experiment, where the water depth (d_w) equaled 0.6 m, the time scale for complete vertical mixing ($=d_w^2/D_V$) was 360 h.

[23] Model calculations made with the best-fit parameter values show that peak breakthrough concentrations were 60 times lower than those calculated assuming conservative advective-dispersive transport (i.e., $\lambda = 0$). The TiO_2 particles were too small to be removed by settling, and the particles did not diffuse to the channel bottom, where they would be susceptible to removal by adsorption to the sediments. There is also no evidence to support particle trapping within stagnation zones as a significant particle removal mechanism because breakthrough-curve tailing, a diagnostic feature of this reversible mass-transfer process, was not observed in our experiment. Interception of particles by aquatic vegetation represented the primary mechanism of particle removal within the surface-water channel.

[24] The effectiveness of the plant stems in scavenging TiO_2 from the water column can be quantified in terms of a single-stem collection efficiency (η_S), which expresses the ratio that particles stick to a single stem to the rate that particles approach a single stem from upstream. Particles are removed from a unit volume of surface water at the rate λC and thus are collected by (stick to) a single stem at the rate $\lambda C(h/P\text{-}\pi hd^2/4)$, where P is the stem density (stems/m^2) and the quantity in parentheses is the volume of water associated with a single (cylindrical) emergent stem of diameter d. The rate at which particles approach the stem is VChd, giving

$$\eta_S = \frac{\lambda}{dV}\left[\frac{1}{P} - \frac{\pi d^2}{4}\right] \tag{4}$$

The η_s value computed with the best-fit estimates of λ and V and with measurements of P ($=1150$ stems/m^2) equals 0.29, indicating that a single stem was capable of scavenging 29% of the particles that approached its projected cross-sectional area from the upstream direction. We suspect that the majority of intercepted particles were bound to periphyton that formed thin coatings on the plant stems. These periphyton sweaters likely provide a substrate favorable for the attachment of most natural inorganic particles of colloid size (i.e., 1 nm to 10 μm) that, like the TiO_2 used in this study, have a net negative surface charge in waters of circumneutral pH.

[25] Our results suggest that migration of colloid-sized mineral particles may be limited to a few tens of meters in

wetlands characterized by laminar flow regimes. Under turbulent flow, particle trapping by wetland vegetation may be comparatively less effective (due to low particle-substrate contact times) and may be reversible (due to elevated shear forces on attached particles). Although the TiO_2 particles should serve as a good analog for other mineral colloids, we caution against using these results to draw inferences about the transport of larger inorganics (e.g., silt), which are susceptible to removal by settling, or colloidal organic matter, which has a relatively lower density and different surface properties. In light of the complex effects that interactions between particle type and flow regime have on particulate-matter transport, we recommend that future research focus on additional model evaluations against field data collected outside the range of conditions studied here.

[26] **Acknowledgments.** This work was funded by the U.S.G.S. We thank Tom Smith for support and Evelyn Gaiser for providing access to the flume.

References

Aumen, N. G., The Role of Flow in the Everglades Ridge and Slough Landscape, in *Science and Restoration of the Greater Everglades and Florida Bay Ecosystem*, 13–14, Palm Harbor, FL, 2003.

Leonard, L. A., and M. E. Luther, Flow hydrodynamics in tidal marsh canopies, *Limnol. Oceanogr.*, *40*, 1474–1484, 1995.

Middleton, B., Hydrochory, seed banks, and regeneration dynamics along the landscape boundaries of a forested wetland, *Plant Ecol.*, *146*, 169–184, 2000.

Nepf, H. M., Drag, turbulence, and diffusion in flow through emergent vegetation, *Water Resour. Res.*, *35*, 479–489, 1999.

Nepf, H. M., et al., A model for diffusion within emergent vegetation, *Limnol. Oceanogr.*, *42*, 1735–1745, 1997a.

Nepf, H. M., et al., The effects of vegetation on longitudinal dispersion, *Estuar. Coast. Shelf Sci.*, *44*, 675–684, 1997b.

Schulz, R., and S. K. Peall, Effectiveness of a constructed wetland for retention of nonpoint-source pesticide pollution in the Lourens River catchment, South Africa, *Environ. Sci. Technol.*, *35*, 422–426, 2001.

J. E. Saiers and S. E. Mylon, School of Environmental Studies, Yale University, New Haven, CT, USA. (james.saiers@yale.edu)

J. W. Harvey, U.S.G.S., Reston, VA, USA.